THE ASTROPHYSICAL JOURNAL, 492:727–742, 1998 January 10

BORON IN LITHIUM- AND BERYLLIUM-DEFICIENT F STARS[1]

ANN MERCHANT BOESGAARD[2,3]
Institute for Astronomy, University of Hawai'i at Manoa, 2680 Woodlawn Drive, Honolulu, HI 96822; boes@galileo.ifa.hawaii.edu
CONSTANTINE P. DELIYANNIS[2,3,4]
Department of Astronomy, Center for Solar and Space Research, and Center for Theoretical Physics, Yale University, P.O. Box 208101, New Haven, CT 06520-8101; con@athena.astro.yale.edu
ALEX STEPHENS[2,3]
Institute for Astronomy, University of Hawai'i at Manoa, 2680 Woodlawn Drive, Honolulu, HI 96822; alex@galileo.ifa.hawaii.edu
AND
DAVID L. LAMBERT
Department of Astronomy, RLM Building 15.308, University of Texas, Austin, TX 78712; dll@astro.as.utexas.edu
Received 1997 April 16; accepted 1997 August 22

ABSTRACT

The Goddard High Resolution Spectrograph (GHRS) has been used with the *Hubble Space Telescope* (*HST*) to observe the B I region at 2497 Å in nine F and G dwarfs of approximately solar metallicity. The stars were selected because they have a variety of Li and Be deficiencies. Most of the nine stars were newly observed at high spectral resolution and high signal-to-noise ratios at the Keck I 10 m telescope, the Canada-France-Hawaii 3.6 m telescope, and the University of Hawaii 2.2 m telescope at 3131 Å for Be II and 6708 Å for Li I. With spectrum synthesis we have determined the abundances of B in our nine program stars and in five other stars from the *HST* archive. The stellar parameters we have used have been determined in a self-consistent way for the program stars and the archive stars. Spectrum synthesis has also been used to determine the Li and Be abundances or upper limits. Corrections to the B and Li abundances due to non-LTE effects have been applied.

The stars originate from the region on the ZAMS of the Li (and Be) dip. In spite of large deficiencies in Li and Be, we find a striking uniformity in the B abundances, i.e., there is no B dip. In all cases the Li deficiency is greater than the Be deficiency. For the coolest and most evolved star in our sample, ζ Her A, the B abundance is 0.6 dex lower than the mean for the other stars. This star also has the largest Be deficiency (more than a factor of 80) and the largest Li deficiency (more than a factor of 600). These data, together with other studies of the Li dip, argue strongly against diffusion and mass loss and in favor of slow mixing as the cause of the Li and Be dip and the absence of a B dip.

Six stars with [Fe/H] from -0.75 to $+0.15$ have Be abundances ranging from the maximum of the sample to a factor of 4 below the maximum, yet these stars have a B/Be ratio that is constant to within ± 0.10 dex and that is close to the predictions of Galactic cosmic-ray spallation of 10–15. The Be range for four stars with solar metallicity is still a factor of 2, and yet the B/Be ratio is constant to within ± 0.03 dex. These results imply that the Galactic cosmic-ray production of B and Be is not uniform relative to the production of elements such as Fe by stellar nucleosynthesis.

Subject headings: nuclear reactions, nucleosynthesis, abundances — stars: abundances — ultraviolet: stars

1. INTRODUCTION

With the *Hubble Space Telescope* (*HST*) and the Goddard High Resolution spectrograph (GHRS), boron (B) joins lithium (Li) and beryllium (Be) as a probe of stellar structure and evolution. In increasing order of stability, Li, Be, and B are all destroyed by proton reactions at temperatures of only a few million degrees in stellar interiors, and hence they survive only in the outermost layers of stars. For example, using a standard solar model (Bahcall & Pinsonneault 1995), we have estimated that the Li, Be, and B preservation regions occupy roughly the outermost 2.5%, 5%, and 20% by mass, assuming no slow mixing below the surface convection zone. These elements can thus probe heretofore poorly understood physical mechanisms that might be important in stellar interiors. Although most previous studies have concentrated on Li alone, because each element survives to a different depth, much more powerful model constraints can be derived when more than one element is considered simultaneously (Deliyannis 1995). In this paper, we focus on the very interesting phenomenon known as the Li dip in F stars. To complement our ongoing studies of Li and Be near the dip, we present here *HST*/GHRS observations of B in Li-deficient F stars and some new observations of Li and Be in the stars observed for B.

Boesgaard & Tripicco (1986a) discovered that Hyades (age $\sim$ 700 Myr) F stars have depleted their surface Li

[1] Based on observations obtained with the NASA/ESA *Hubble Space Telescope* through the Space Telescope Science Institute which is operated by the Association of Universities for Research in Astronomy, Inc., under NASA contract NAS5-26555.

[2] Visiting Astronomer, W. M. Keck Observatory, jointly operated by the California Institute of Technology and the University of California.

[3] Visiting Astronomer at the Canada-France-Hawaii Telescope operated by the National Research Council of Canada, the Centre National de la Recherche Scientific of France, and the University of Hawaii.

[4] Beatrice Watson Parrent Fellow, Institute for Astronomy, University of Hawaii at Manoa; Hubble Fellow.

abundance. In particular, stars within the $T_{\rm eff}$ range 6400–6800 K exhibit dramatic Li underabundances. In addition, Be, which is sturdier than Li, is also affected, for some severely Li-depleted stars are also known to be Be depleted (Boesgaard 1976). Every sufficiently old cluster that has been observed shows this Li dip (Balachandran 1995) as do field stars (Boesgaard & Tripicco 1986b). Since Pleiades (age $\sim$70 Myr) stars show (nearly) no Li depletion (Pilachowski, Booth, & Hobbs 1987; Boesgaard, Budge, & Ramsay 1988; Soderblom et al. 1993), the Li dip develops during the main sequence and not before. The surprising discovery of a Li dip blatantly contradicted the predictions of the standard stellar evolution theory. Already by the time model stars arrive on the zero-age main sequence (ZAMS), Li is preserved only in the outermost few percent of the mass, and the surface convection zone occupies a much smaller region (Deliyannis & Pinsonneault 1993). Hence, there is no way to affect the surface Li abundance in these models as, for example, might be the case in stars of significantly lower mass (e.g., K stars), where Li burning can occur at the base of a much deeper convection zone.

To explain the Li dip, proposed physical mechanisms beyond those incorporated into the standard model have proliferated. These include mass loss (Schramm, Steigman, & Dearborn 1990), microscopic diffusion (Michaud 1986; Richer & Michaud 1993), and various forms of slow mixing. The latter include mixing caused by gravity waves (García-López & Spruit 1991; Montalban & Schatzman 1996), meridional circulation (Charbonneau & Michaud 1988), turbulent diffusion and mechanisms related to meridional circulation (Vauclair 1988; Charbonnel et al. 1994), and rotationally induced mixing related to the onset of instabilities that cause angular momentum transport (Pinsonneault, Kawaler, & Demarque 1990; "Yale" models).[5] Discerning which of these, if any, is the dominant mechanism responsible for the creation of the Li gap is interesting not only for advancing our knowledge of stellar interiors, but possibly also for cosmology. For example, helium diffusion in the outer layers might reduce globular cluster ages by as much as 25% (Deliyannis, Demarque, & Kawaler 1990; Profitt & Vandenberg 1991; Chaboyer et al. 1992). Slow mixing might imply a significantly higher primordial Li abundance, with implications for constraining models of big bang nucleosynthesis (BBN) and (in the context of a particular BBN model) for the nature of dark matter (Deliyannis 1990; Chaboyer & Demarque 1994; Deliyannis, Boesgaard, & King 1995).

We expound on the possible implications for primordial Li, as most of the various models that incorporate rotation-related instabilities predict an intimate connection between the halo dwarf Li depletion, disk dwarf Li depletion, and the Li gap. Although this is often ignored in discussion of the halo Li plateau, open clusters also exhibit a Li plateau, in approximately the same $T_{\rm eff}$ range as the halo Li plateau. Progressively older open clusters appear to have lower mean Li abundance values for this plateau, with the halo Li plateau being the lowest (Boesgaard 1991; see also Figs. 1 and 2 in Ryan & Deliyannis 1995 for the progression from the Pleiades to the Hyades to M67 to intermediate-metallicity stars to halo stars). The models would predict that this is a result of slow mixing acting over time, which depletes (on average) the whole plateau. In these models, the halo Li plateau (and its depletion) is completely analogous to the open cluster Li plateau, and the Li gap is a natural extension of this mixing to slightly higher mass stars. Conversely, it could be argued that the plateaus are merely reflecting Galactic Li production with time from a (low and essentially undepleted) halo Li plateau. (Of course, it is also possible that both Li plateau depletion and Galactic Li production have occurred.) However, there is evidence that the Hyades and M67 Li plateaus have indeed been depleted from some higher value. This evidence takes the form of higher than average Li abundances in short-period binaries in these clusters (Ryan & Deliyannis 1995; Deliyannis et al. 1994); better than average Li preservation in such binaries was specifically put forth as a test of the Yale (Deliyannis 1990) and other rotational (Zahn 1994) models. While these provocative indications do not directly prove that the halo Li plateau is depleted, they do underscore the possible implications for interpreting BBN, and encourage further study of slow mixing in low-mass stars. For additional reviews and discussions of some tests of models with slow mixing, see Deliyannis (1995), King, Deliyannis, & Boesgaard (1997a), and Pinsonneault (1997).

By itself Li can potentially be used to decipher the physical cause of the Li gap. For example, see the discussion in Balachandran (1995), who has reviewed the observational database for the morphology of the Li-$T_{\rm eff}$ relation near the Li gap in open clusters. One test exploits the fact that each proposed mechanism leaves a different profile (with depth) of Li preservation region. Li data in M67 subgiants that have evolved out of the Li gap can reveal these profiles and have been used to argue strongly against diffusion and weakly against mass loss (Deliyannis, King, & Boesgaard 1996). These M67 data support slow mixing.

More powerful constraints can be realized when Li and Be are considered together. While each proposed mechanism might create a Li gap, the effects on Be differ (Deliyannis & Pinsonneault 1993). In the case of mass loss, Be should be unaffected; in the case of diffusion, Li and Be should diffuse at similar rates for $T_{\rm eff} < 6600$ K; in the case of slow mixing, Li and Be should deplete simultaneously, with Li being depleted more severely, where the exact Li/Be ratios depend on how the mixing occurs. Deliyannis & Pinsonneault (1993) especially emphasized the importance of the star 110 Her, which exhibits Li and Be depletion factors of 100 and 10, respectively (Boesgaard & Lavery 1986). This pattern, if typical, argues strongly against mass loss and diffusion and strongly favors slow mixing. Subsequent studies have shown that 110 Her is not an isolated anomaly (Stephens et al. 1997).

Boron is more resistant to protons than either Li or Be. The complementary information from B observations can thus potentially provide additional, very powerful constraints. For example, diffusion would predict large B variations to accompany the observed Li and Be variations; mass loss would demand that all the Be be gone before B depletion begins; slow mixing would allow both Be and B to be depleted, though Be much more strongly, again depending on how the mixing occurs. The purpose of the present study is to add observations of B to the picture, to use our derived ratios of Li/Be, Li/B, and Be/B to test

[5] The Yale models are an attempt to model stellar rotation and its implications for stellar structure and evolution; they were *not* constructed specifically with the goal of explaining the Li gap, although they do predict it.

further the conclusions reached in the above studies, and to seek even stronger constraints for the models.

2. OBSERVATIONS

2.1. *Selection of Stars*

We have selected a sample of stars with various levels of Li and Be deficiencies. An F7 dwarf with nearly normal Li and Be, ϕ^2 Cet, is our standard. One star, HR 962, has depleted but detectable Li and Be. Three others, HR 244, HR 6541, and θ Cyg, are very Li depleted with upper limit Li abundances but have detectable Be features. One cooler star, ζ Her A, was included because it is severely depleted in both Li and Be.

Light-element depletion is predicted and observed to be a strong function of metallicity (see, e.g., Ryan & Deliyannis 1995). We thus included the somewhat metal-deficient stars σ Boo and σ Peg which have no Li lines and barely detectable Be lines. We also observed HR 4501, which shows no Li or Be lines in its spectrum.

In addition to our sample, we include B spectra of stars from the *HST* archive: θ UMa, ι Peg, and α CMi from Lemke, Lambert, & Edvardsson (1993) and χ Her and HD 184499 from Duncan et al. (1997b). The positions of our stars in the H-R diagram as well as those from the archive are shown in Figure 1. The temperatures were determined as described in § 3. The absolute magnitudes come from Strömgren photometry, c_1 and Hβ, and the prescription in Boesgaard & Tripicco (1986b) with the standard relations for $c_1(\beta)$ and M_v(ZAMS,β) from Crawford (1975). The luminosities plotted in Figure 1 were derived after application of appropriate bolometric corrections.

The stellar evolutionary tracks shown are part of the new Yale isochrone program (P. Demarque 1997, private communication). They have been constructed with a solar-calibrated mixing length (1.7), and they incorporate Livermore OPAL opacities (Iglesias & Rogers 1991; Rogers & Iglesias 1994). The models also have assumed a core overshoot by 0.1 pressure scale heights, which affects the shape near the turnoff, as emphasized by Maeder (1976). Such a small amount of overshoot produces superior fits to the color-magnitude diagrams of clusters that have turnoffs in this part of the H-R diagram (see, e.g., Dinescu et al. 1995; Kozhurina-Platais et al. 1997).

2.2. *Hubble Space Telescope Boron Observations*

Abundances of B can be determined for F and G stars from the B I resonance line near 2500 Å. For two of the brightest stars, HR 244 and ζ Her, we used the high-resolution grating on the GHRS, ECH-B, and for the remainder, we used G270M. The resolution at 2500 Å with ECH-B is 80,000 and with G270M is 26,000. The integration times ranged from 13 to 55 minutes, and the signal-to-noise ratios (S/N) per diode (where at FWHM there are six diodes for G270M and 16 for ECH-B) range from 12 to 60. These observations are presented in Table 1, in which we

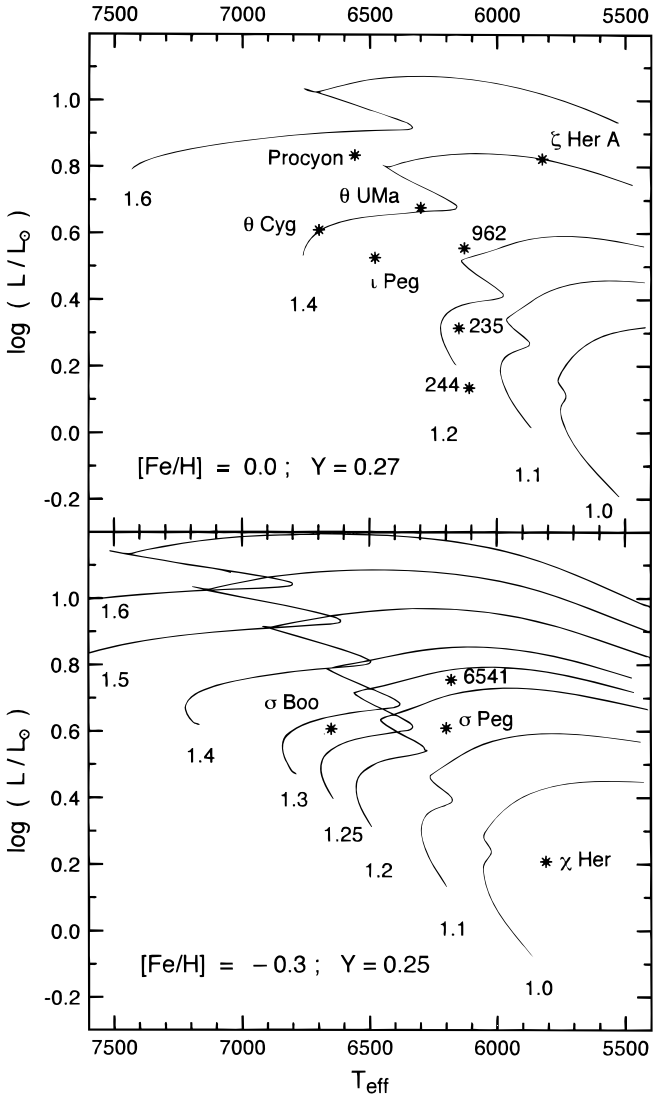

FIG. 1.—H-R diagrams showing the positions of our stars. The evolutionary tracks are from the Yale models (see text). The upper panel is for solar metallicity and the lower for [Fe/H] = −0.3.

TABLE 1

BORON OBSERVATIONS

Star	HR Number	HD Number	V	$B-V$	$U-B$	Integration Time (s)	Diffraction Grating	Signal-to-Noise Radio per Line Width
ϕ^2 Cet.....	235	4813	5.19	+0.51	+0.00	870	G270M	81
... .	244	5015	4.80	+0.54	+0.09	3264	ECH-B	48
94 Cet.....	962	19994	5.07	+0.57	+0.11	870	G270M	54
62 UMa.....	4501	101606	5.75	+0.44	−0.11	870	G270M	61
σ Boo	5447	128167	4.46	+0.36	−0.08	870	G270M	125
ζ Her A	6212	150680	2.81	+0.64	+0.21	762	ECH-B	56
... .	6541	159332	5.66	+0.49	+0.00	870	G270M	59
θ Cyg.....	7469	185395	4.48	+0.38	−0.03	979	G270M	145
σ Peg.....	8697	216385	5.16	+0.48	−0.02	870	G270M	73

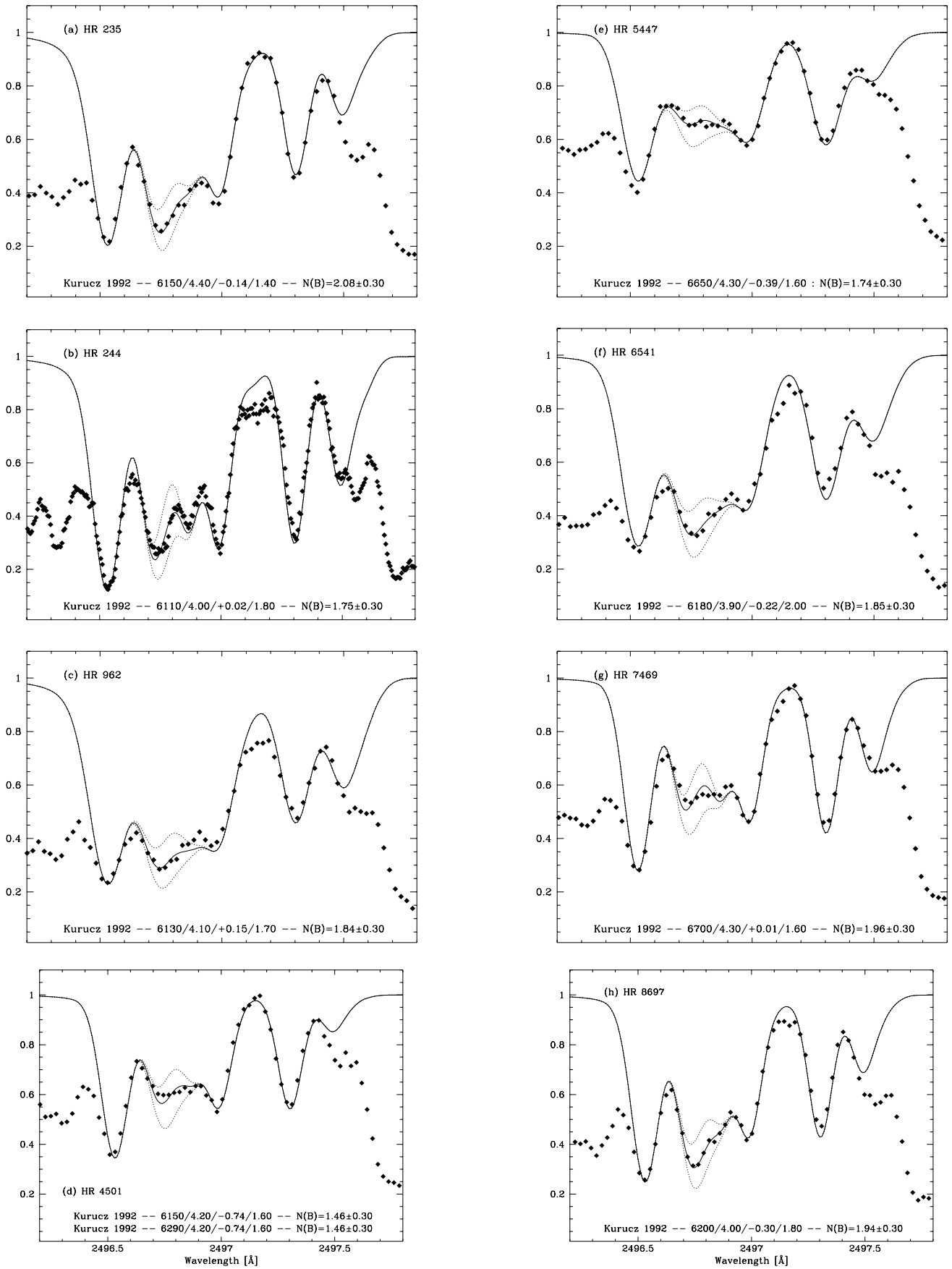

FIG. 2.—Observed spectra for eight of our stars in the B I region shown as diamonds. The best-fit synthetic spectra are shown as solid lines, while dotted lines show the B abundances a factor of 2 above and below the best fit.

TABLE 2

BERYLLIUM OBSERVATIONS

HR Number	Telescope	UT Date	Time (minutes)	Signal-to-Noise Ratio
235	CFHT (G)	1995 Oct 16	15	75
244	Keck	1993 Oct 5	5	98
962	Keck	1993 Oct 5	5	118
2943	Keck	1993 Oct 7	1	400
3775	Keck	1994 Mar 1	3	95
4501	CFHT (8)	1991 Apr 4	30	63
5447	Keck	1995 Mar 14	3	160
6212	Keck	1994 Jul 5	6	215
6541	CFHT (8)	1991 Apr 4	20	47
7469	CFHT (G)	1995 Oct 16	6	53
8697	CFHT (G)	1995 Oct 15	10	90

give star names, HR numbers, and HD numbers. Hereafter we will refer to the stars by their names or HR numbers. The S/N ratios given in Table 1 are per line width (FWHM) rather than per diode. Samples of the B spectra are shown in Figure 2; these figures will be discussed more in §§ 3 and 4.

2.3. *Keck and CFHT Beryllium Observations*

Abundances of Be come from observations of the Be II resonance lines near 3130 Å; the wavelength of this doublet is near the atmospheric cutoff so it is helpful to perform such observations at Mauna Kea. During twilight and cloudy times on other programs, we were able to make Be observations with HIRES on the Keck I 10 m telescope for four of our *HST* program stars and for two stars that had been observed for B by Lemke et al. (1993): θ UMa = HR 3775 and Procyon = α CMi = HR 2943. The detector was a 2048^2 Tektronix CCD. The nominal resolution is 48,000, and the effective pixel size is 0.022 Å. Three of our stars were observed for Be with the Canada-France-Hawaii 3.6 m telescope with the f/4 coudé GECKO spectrograph [CFHT(G)] and the UV-sensitive mirror train and the UV-sensitive Orbit CCD (QE of 80% at 3130 Å). The resolution is 120,000, and the dispersion is 0.010 Å pixel^{-1}. For two stars, we relied on previous spectra obtained with CFHT and the f/8 coudé spectrograph [CFHT(8)] presented by Stephens et al. (1997). These spectra have a dispersion of 0.067 Å pixel^{-1}. The Be observations, dates, exposure times and signal-to-noise ratios are given in Table 2. Examples of the CFHT GECKO spectra are shown in Figure 3 and will be further discussed in §§ 3 and 4.

TABLE 3

LITHIUM OBSERVATIONS

HR Number	Telescope	UT Date	Time (minutes)	Signal-to-Noise Ratio
244	UH 2.2 m	1992 Aug 17	40	420
	UH 2.2 m	1993 Mar 8	60	455
	UH 2.2 m	1993 Oct 4	210	620
962	UH 2.2 m	1992 Aug 17	46	420
	UH 2.2 m	1993 Mar 7	40	335
2943	UH 2.2 m	1992 Aug 17	2	480
4501	Keck	1996 Jun 6	6	1100
5447	UH 2.2 m	1993 Jun 6	80	460
6212	UH 2.2 m	1992 Aug 19	10	600
	UH 2.2 m	1993 Jun 6	80	1300
6541	UH 2.2 m	1993 Mar 8	60	300
	Keck	1996 Jul 25	18	1590
8697	UH 2.2 m	1992 Aug 17	14	70
	UH 2.2 m	1992 Aug 18	40	315
	UH 2.2 m	1993 Oct 31	30	90
	UH 2.2 m	1993 Nov 1	120	600
	Keck	1996 Jul 25	12	1320

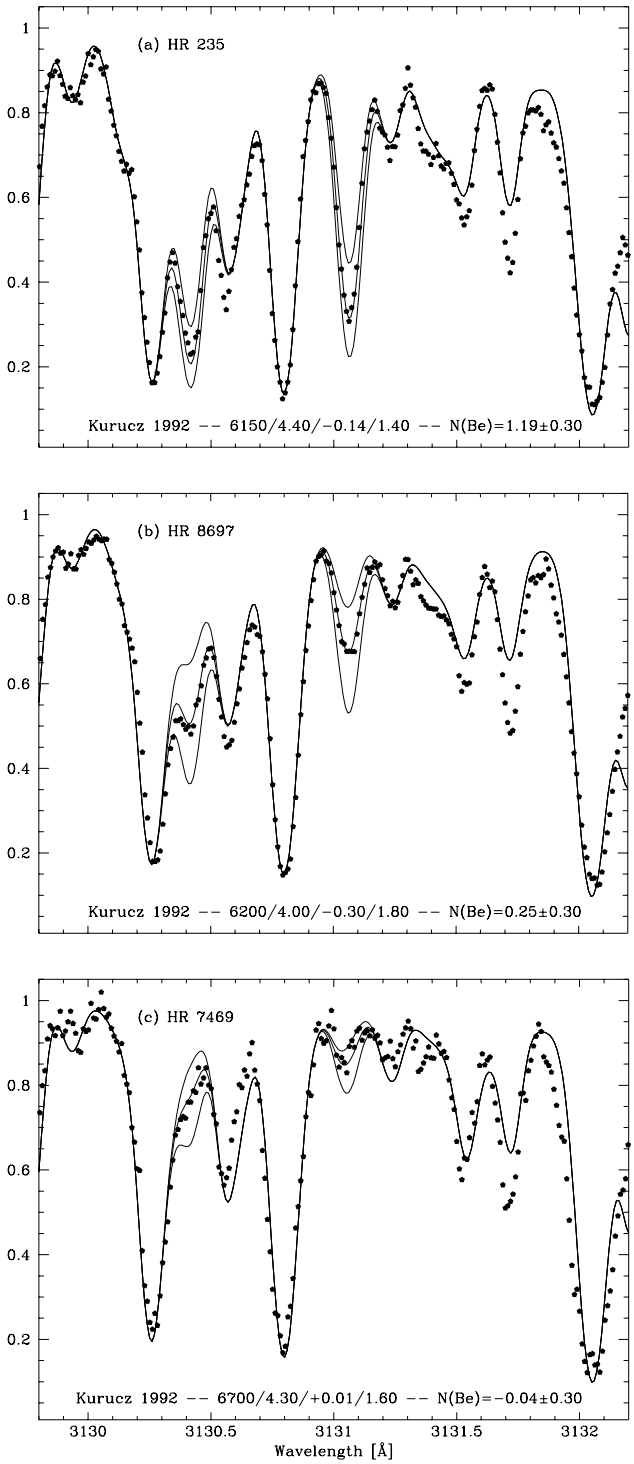

FIG. 3.—Samples of the Be spectra from the CFHT GECKO spectrograph for HR 235, HR 8697, and HR 7469, shown as pentagons. The solid lines are the best-fit Be synthetic spectra, and a factor of 2 above and below the best fit. HR 235 shows nearly normal Be, while HR 8697 is depleted by 1.12 dex and HR 7469 by 1.53 dex.

2.4. *Keck and UH 2.2 Meter Lithium Observations*

Abundances of Li can be determined from the Li I resonance line at 6707 Å. Again during twilight and cloudy hours, we were able to obtain observations of three of the

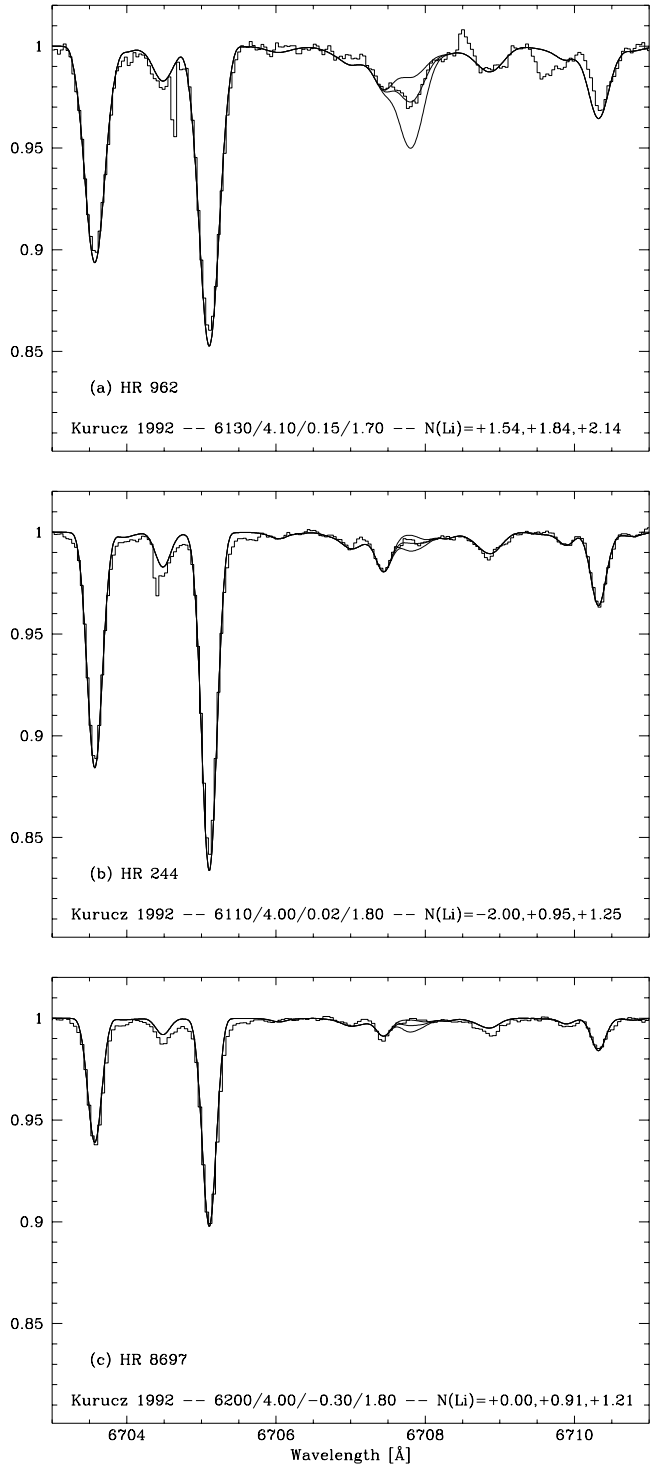

FIG. 4.—Samples of the Li spectra for HR 962 and HR 244 (from UH 88 inch [2.23 m] coudé spectrograph) and HR 8697 (from Keck I + HIRES), shown as histograms. The synthetic spectra are solid lines with the best fit in the middle, a factor of 2 higher Li abundance as the lower line, while the uppermost line corresponds to a considerably lower Li abundance for HR 244 and HR 8697. Only in HR 962 do we detect a Li line. The others are conservative upper limits.

HST stars with the Keck I 10 m telescope with HIRES. The spectra cover the range 4480–6770 Å with some gaps between the orders. At 6700 Å the dispersion is 0.047 Å pixel^{-1}. As part of a large Li survey at high resolution and high signal-to-noise ratio, we have made observations with the longest focal length (192 inch [4.8 m]) coudé camera at the UH 2.2 m telescope. Those spectra have a resolution of $\sim$70,000 and a dispersion of 0.040 Å pixel^{-1}. The detector was a Tektronix 2048^2 CCD. Multiple spectra were obtained of these stars and co-added, sometimes over several observing runs. Table 3 gives the details of the Li observations including the dates, exposure times, and signal-to-noise ratios. Figure 4 shows some examples of the Li region spectra, which will be discussed more in §§ 3 and 4.

3. DATA REDUCTION

3.1. *Boron*

The *HST* calibrated, or pipelined, FP-SPLIT GHRS data, as well as the accompanying error images, were combined using the IRAF STSDAS tasks *poffsets*, *specalign*, and *resample*. Thus multiple exposures, acquired at slightly different grating settings to minimize errors associated with photocathode irregularities, were co-added and placed on a linear wavelength scale. Because we are primarily concerned with a 1 Å window centered on the "blue" feature of the B I resonance doublet ($\lambda \sim 2946.8$ Å), we simply divided both the flux-calibrated science and error images by a constant value to place each on a relative intensity and error scale. While the UV continuum certainly is not constant over large wavelength intervals in these cool dwarfs, variations over the 1 Å interval of interest here should be negligible. The signal-to-noise ratio (S/N) of each fully calibrated and co-added spectrum was estimated using both the raw, observed signal and the assumption that photon counting errors are the dominant source of uncertainty in a measured flux. These empirical estimates of the per-pixel, or quarter-stepped diode, S/N reveal that the *HST* pipeline error images accurately reflect the uncertainty in the number of counts recorded by an individual detector element. Examples of the fully reduced B spectra are shown in Figure 2.

3.2. *Beryllium*

Observations of the Be II resonance doublet were conducted as part of a survey for Be in the atmospheres of Li-deficient F and G stars. Most of the Be II data, acquired using two different coudé spectrographs at the Canada-France-Hawaii telescope, were reduced using the basic image processing tools bundled with the NOAO IRAF package. Explicit details of the CFHT reductions are presented elsewhere (Boesgaard & King 1993; Stephens et al. 1997), but some examples of fully calibrated CFHT GECKO spectra are shown in Figure 3. Data acquired using the 10 m W. M. Keck telescope and the High Resolution Echelle Spectrograph were processed in a slightly different but, on the whole, similar manner.

3.3. *Lithium*

Spectra of the Li I resonance doublet were collected as part of a systematic search for Li in the photospheres of cool stars. The data from each of the four UH observing runs were reduced in a self-consistent fashion. Standard IRAF tasks were used to subtract any bias or scattered light contaminant, excise cosmic rays, and flatten all of the raw science images. These preprocessed, two-dimensional spectra were then aperture extracted and wavelength rectified using nightly Th-Ar frames. If multiple exposures were acquired of a particular object, the individual one-dimensional frames from each night were combined. Subsequently, the co-added spectra from different runs were combined. These fully reduced spectra were then placed on

a relative intensity scale using a low order Legendre polynomial, resulting in the spectra shown in Figure 4.

The general recipe used to reduce the UH spectra was also applied to the reduction of the Keck + HIRES Li data; however, one extra task was performed in addition to the traditional preprocessing steps (overscan subtraction, trimming, flat-fielding, etc.). Bias subtraction was included because each night several zero-second images, which mapped a weak, nonuniform signal, were acquired. Extraction of the preprocessed spectra required use of IRAF ECHELLE tasks specifically designed to reduce multiple-order echelle spectra. Each order was aperture extracted using *apall*; furthermore, to ensure that any scattered background light was removed prior to extraction, residual flux away from the stellar PSF but still within the 7″ long slit was subtracted. These extracted spectra were placed on a linear wavelength scale and co-added if multiple exposures existed. Each science image therefore resulted in 29 spectral orders spanning 4500–6800 Å. Only the order containing the Li I resonance doublet is considered here, and an example of a fully reduced Keck, Li spectrum is shown in Figure 4*c*.

4. ANALYSIS

4.1. *Stellar Parameters*

The inferred element abundances are sensitive to the choice of stellar parameters, and any systematic errors in the adopted effective temperature ($T_{\rm eff}$), surface gravity (log g), microturbulence velocity (ξ), and metallicity ([Fe/H]) will necessarily translate into imprecise abundance estimates. The parameters were newly determined in a self-consistent manner for both our program stars and the *HST* archive stars.

Iron abundances were taken from the catalog of Taylor (1994b, 1995), a homogenized compilation of literature [Fe/H] values published prior to 1993. The adopted uncertainty in the each metallicity was conservatively chosen to be 0.10 dex.

The effective surface temperature of each star was calculated using an average of eight photometric scales and, when available, an estimate based on Infrared Flux Measurement (IRFM) techniques. The Magain (1987) $(b-y)$ and $(B-V)$ scales were used in conjunction with the Saxner & Hammärback (1985) $(b-y)$, H_β, and $(B-V)$ calibrations. Literature averages from Taylor (1994a, 1995) for $\Theta_{(R-I)}$ were also used. The star HR 5447 has published effective temperatures based on the Carney (1982) $(V-K)$ scale; furthermore, both HR 5447 and HR 7469 were included in the survey of Blackwell & Lynas-Gray (1994), which utilized the IRFM to estimate surface temperature. A straight average of each of the available $T_{\rm eff}$'s results in the temperatures listed in Table 4. While the standard deviation of the mean for an individual star was, on average, 50 K, we adopt twice this amount as a conservative measure of the uncertainty in the calculated effective temperatures. By adopting the mean of several temperature scales as the $T_{\rm eff}$ for our program stars, systematic errors associated with any particular calibration may average out.

Deviations from the Crawford (1975) empirical c_1-Hβ ZAMS served as measure of the surface gravity in our stars. Armed with effective temperatures, metallicities, and Strömgren photometry, we assessed the surface gravity for each of our sample stars using the recipe developed by Edvardsson et al. (1993). The results of this calculation are listed in Table 4. The 1 σ log g uncertainty, here estimated to be 0.20 dex, arises from both random photometric errors and systematic errors associated with the choice of empirical ZAMS relationship (Edvardsson et al. 1993).

Microturbulence velocities were calculated using the Nissen (1981) prescription, which is a function of both the adopted $T_{\rm eff}$ and surface gravity. We characterize the uncertainty in this calculation by fully propagating the individual $T_{\rm eff}$ and log g uncertainties through the Nissen equation. The calculated 1 σ error in ξ, 0.25 km s^{-1}, was used to gauge the relative uncertainty in a boron abundance due to changes in the adopted microturbulence.

The parameters adopted for our *HST* program stars are given in Table 4.

Our Keck spectra of HR 4501 revealed that it is a double-lined spectroscopic binary confirming several reports based on speckle interferometry that HR 4501 is a double star system (Bonneau et al. 1986; Blazit, Bonneau, & Foy 1987). We determined temperatures for each component by measuring the equivalent widths of the Fe I 6703 and 6705 Å lines and using the empirical relationship of Boesgaard & Tripicco (1986b), which relates the ratio of $W(6703)/W(6705)$ to $T_{\rm eff}$. We also determined the Fe abundances in both stars using five Fe I lines. The measured equivalent widths, of course, were scaled to reflect each star's differing contribution to the continuum flux. The derived value for this system is [Fe/H] = −0.74, which compares well with −0.82 found by Boesgaard & Tripicco (1986b) who treated it as a single star. The two components have very similar temperatures: 6150 and 6290 K. While HR 4501 has no detectable Li or Be lines, the double star nature was taken into account when estimating Li and Be upper limits. For B

TABLE 4

STELLAR PARAMETERS AND LIGHT-ELEMENT ABUNDANCES

HR Number	HD Number	log g	$T_{\rm eff}$	[Fe/H]	ξ	log N(Li)[a]	log N(Li)$_N$[b]	log N(Be)[a]	log N(B)[a]	log N(B)$_N$[b]	B/Be
235.....	4813	4.40	6150	−0.14	1.40	+2.76	+2.71	+1.19	+2.08	+2.18	9.8
244.....	5015	4.00	6110	+0.02	1.80	≤ +0.95	≤ +0.94	+0.33	+1.75	+1.85	33
962.....	19994	4.10	6130	+0.15	1.70	+1.84	+1.83	+0.91	+1.84	+1.91	10
4501.....	101606	4.20	6210	−0.74	1.60	≤ +1.21	≤ +1.20	≤ −0.34	+1.48	+1.74	≥120
5447.....	128167	4.30	6650	−0.39	1.60	≤ +1.40	≤ +1.35	−0.26	+1.74	+2.03	195
6212.....	150680	3.78	5825	0.00	1.50	≤ +0.50	≤ +0.50	≤ −0.50	+1.40	+1.47	≥93
6541.....	159332	3.90	6180	−0.22	2.00	≤ +0.90	≤ +0.89	+0.12	+1.85	+2.00	76
7469.....	185395	4.30	6700	+0.01	1.60	≤ +0.34	≤ +0.34	−0.11	+1.96	+2.15	182
8697.....	216385	4.00	6200	−0.30	1.80	≤ +0.91	≤ +0.90	+0.25	+1.94	+2.09	69

[a] LTE abundances.
[b] Non-LTE abundances.

we constructed two individual syntheses with parameters appropriate to the individual stars. We then combined the two syntheses, weighting each according to each star's contribution at 2500 Å.

In a recent study of ζ Her, Chmielewski et al. (1995) derive parameters for the two stars in this system; the secondary is 2.6 mag fainter than the primary and about 500 K cooler. We find that the secondary may contribute 5% at the B wavelength, 6% at Be, and 8% at Li. In our Li spectrum with S/N = 1430, we see no evidence for any spectral features of the secondary, even though the lines of CN and Fe I would be relatively stronger in the cooler star. For this star, we constructed syntheses for each component and combined them according to the relevant percent contribution at Li, Be, and B. This results in a B abundance that is 0.02 dex lower than treating it as a single star. The limits on Be and Li are $\sim$0.1 dex lower.

4.2. *Abundances*

To determine the number of Li, Be, and B atoms present in the photospheres of our program stars, we used the stellar line analysis package MOOG (Sneden 1973) in conjunction with model atmospheres and modern atomic data to create synthetic spectra that roughly reproduce our observations. R. L. Kurucz (1992, private communication) calculated model atmospheres, which discretely span a space of $T_{\rm eff}$, log g, and [Fe/H], using realistic opacities and the standard, mixing-length treatment of convection. We interpolated between grid points in this Kurucz model lattice to produce synthetic atmospheres with properties similar to our program stars. "Line lists," which contain information regarding an absorber's ionization state, rest wavelength, oscillator strength, and excitation potential and are needed to manufacture artificial spectra, were obtained from the literature.

While the condition that the atmosphere be in local thermodynamic equilibrium (LTE) was explicitly assumed in all abundance calculations, there is no guarantee that the Li, Be, and B resonance lines do, in fact, form in layers characterized solely by local processes. However, rather than run non-LTE syntheses for each star, we model the resonance lines, and all surrounding absorption features, as being formed in regions characterized by LTE. If necessary, corrections to the LTE abundances are performed to compensate for nonlocal phenomena.

4.2.1. *Boron*

Boron abundances were estimated by creating synthetic spectra and adjusting the number of B absorbers until the reduced chi-squared statistic (χ^2_ν) between the synthetic spectrum and the observed data reached a minimum. Instead of modeling the "red" B I feature, which is severely contaminated by neighboring strong lines, we concentrated on replicating a 1 Å window (2496.5–2497.5 Å) surrounding the less-blended "blue" B I 2496.8 Å resonance line. A list of absorption lines compiled by Duncan et al. (1997a) served as the primary source of atomic data. This list was drawn, ultimately, from the expansive database of electronic transitions amassed by R. L. Kurucz (1993) and then adjusted to match a variety of observed dwarf and giant star spectra. In particular, Duncan et al. utilized $\sim$20 lines with observed or semiempirical wavelengths and oscillator strengths to reproduce archival spectra of Procyon (HR 2943) and HD 140283. Since we are concerned with near-solar metallicity disk stars, we also attempt to reproduce a GHRS ECH-B Procyon spectrum originally observed by Lemke et al. (1993). Using the method outlined in the preceding sections, we calculated a slightly different complement of stellar parameters for Procyon; consequently, adjustments to the absorption oscillator strengths, or *gf*-values, were necessary if the spectrum of HR 2943 was to be reproduced. We did not rely solely on Procyon as a benchmark, though. Indeed, the one of the coolest stars in our sample (HR 235) was also used to constrain the *gf*-value alterations. To reproduce both the F- and G-star data required lessening the oscillator strength of several Fe-peak lines neighboring the blue B I transition. Reducing the *gf*-values will necessarily require a larger number of boron atoms to compensate for the decreased strength of the adjoining absorption features; nevertheless, these *gf*-value adjustments provide a marked improvement in the general fit between the synthetic spectra and the observed data. Details of the line list adjustments are as follows: The oscillator strengths of a Co I feature (λ = 2496.708) and three Fe I lines were decreased. The Co I *gf*-value was reduced by a factor of 1.6, while the 2496.533 Å, 2496.869 Å, and 2496.992 Å Fe I lines were diminished by 1.8 times, 1.7 times, and 2.8 times, respectively. Syntheses were then created, and boron concentrations estimated, for our entire sample using this updated line list. Lemke et al. (1993) note that the choice of the van der Waals C_6 parameter is key to reproducing the observed spectra. We used the classical Unsöld (1955, pp. 326 and 331) formula to calculate the damping parameter for each of the included transitions.

The spectra in Figure 2 show eight of our stars along with the best synthetic spectrum fit and two "error bar" spectra. The high and low error bar models represent a factor of 2 decrease and increase in the best-fit abundance. Again, while the *gf* adjustments alter the relative strength of the Fe-peak lines surrounding the blue feature of the B I resonance doublet, the alterations require more boron atoms to reproduce the observed spectra. Thus, the LTE B abundances may be thought of as a conservative overestimate of the boron content in the atmospheres of our program stars. These best-fit B abundances are given in the tenth column of Table 4, while non-LTE B values, calculated using the routines described in Kiselman (1994) and Kiselman & Carlsson (1994), are listed in the eleventh column of the same table.

4.2.2. *Beryllium*

The line list of King et al. (1997a) was utilized to replicate a small window of UV wavelength space surrounding the Be II resonance doublet. Slight adjustments to this list were made by Stephens et al. (1997) in order to replicate better the spectra of F stars that are of primary interest here.

In Figure 3 we show the Be region spectra of three stars along with the best synthetic spectrum fit and Be abundances a factor of 2 above and below this value. The Be abundances are given in the ninth column of Table 4. Non-LTE effects are very small for the Be II lines; the actions that overpopulate a level and those that underpopulate it cancel each other out (Kiselman & Carlsson 1994; García-López, Severino, & Gomez 1995); hence, we report only LTE Be abundances.

4.2.3. *Lithium*

An extensive line list containing data for several hundred absorption features between 6703 and 6711 Å, compiled by

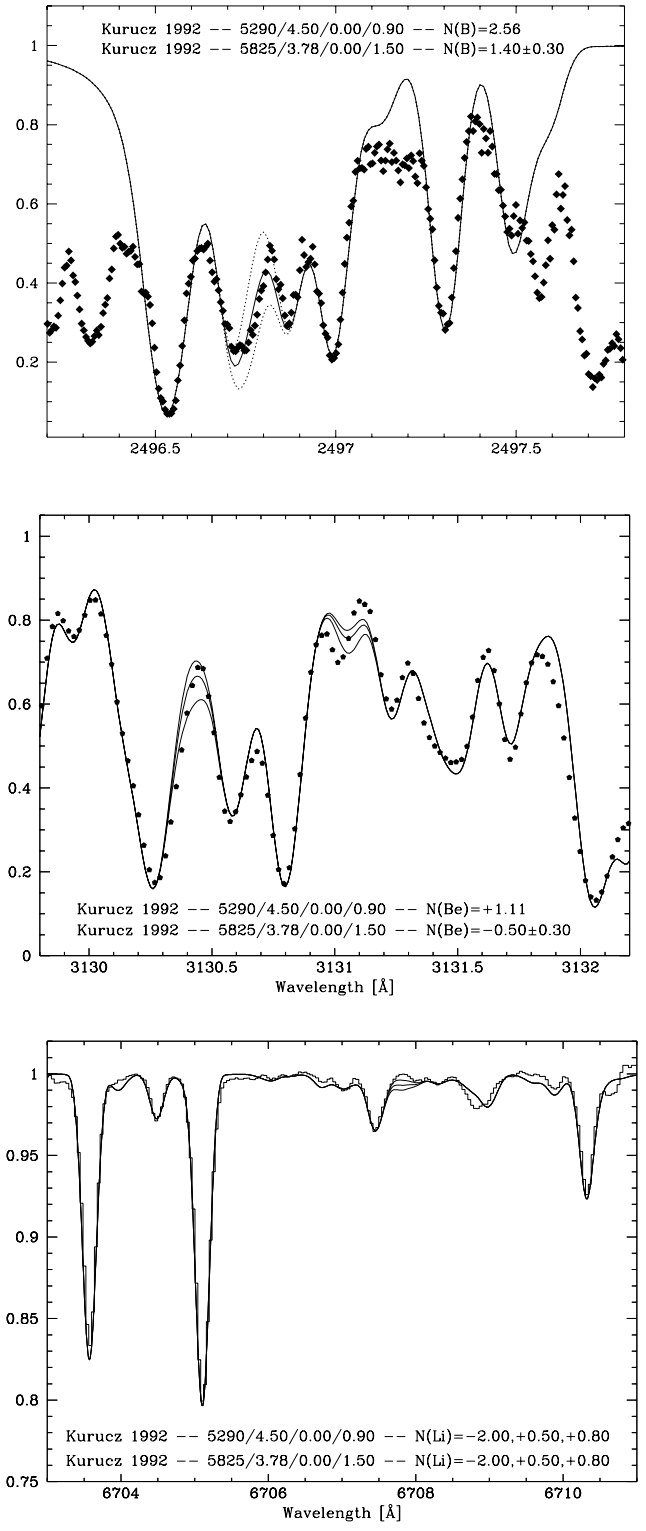

FIG. 5.—Observed and synthesized spectra of B, Be, and Li in ζ Her A, the coolest star in our sample. Boron is detected but depleted, but Be and Li are upper limits, lower than the meteoritic abundances by at least 1.9 dex and 2.8 dex, respectively. The parameters of the two stars are given in the figure title.

Hiltgen (1996) and fine-tuned to match the Sun and a variety of other stars by King et al. (1997b), was used to model the Li region. No alterations to that line list were made; the general agreement between the synthetic spectrum and the observed data was quite good.

Figure 4 shows the Li region of three stars and synthetic spectrum fits. Only HR 962 has a detectable Li line. The best-fit synthesis reveals a Li abundance of 1.84, while the two surrounding syntheses represent a factor of 2 increase and decrease in this abundance. For HR 244 and HR 8967, we choose the middle fit as a conservative Li upper limit. The lower line represents a factor of 2 more Li, while the upper lines are for considerably lower Li abundances. These results are given in the seventh column in Table 4. We have used the Carlsson et al. (1994) routines to find the non-LTE Li abundance, which is given in the eighth column in Table 4.

4.2.4. ζ *Her*

One of our stars, ζ Her, was selected because of its extraordinary depletions in Li and Be and deserves special notice here. In Figure 5 we show the Li, Be, and B regions of this star and the synthetic spectra for each element. The Li deficiency could be extremely severe, possibly 5 orders of magnitude or more relative to the meteoritic value. In this cool star there is an unidentified line near the Be II λ3131 line that is not present in the warmer stars so we can not make as low an assessment of Be; nonetheless, it is deficient by a minimum of nearly 2 orders of magnitude relative to the meteoritic value. Of our program stars, ζ Her has the lowest B abundance.

4.3. *Error Analysis*

While the presence of unknown systematic errors may place the *absolute* boron abundances on a slightly different scale than other works, great care was taken to ensure that abundances were calculated in a self-consistent fashion. Stellar parameters were either taken from a similar source or calculated using the procedures described above. Furthermore, only one line list was used to manufacture synthetic spectra. Thus the *relative* differences between our program stars' superficial B abundances should reflect real, quantitative differences in the photospheric boron abundances. However, making secure statements regarding B depletions also requires understanding the errors associated with a calculated B abundance. Thus, the input parameters needed to secure a photospheric B concentration were individually varied by $\pm 1\ \sigma$ to test the effect each quantity had on the resultant B abundance. A new synthetic spectrum, reflecting the altered input parameter, was created, and the number of boron absorbers was either increased or decreased in 0.01 dex steps until the reduced χ^2 statistic between the GHRS data and the artificial spectra reached a minimum.

As is listed in Table 5, increasing the temperature of the stellar models by 100 K required raising the boron abundance as well since the Fe-peak lines that border the blue B I feature are weaker at higher temperatures. Lowering the $T_{\rm eff}$ had an opposite effect. However, increasing (decreasing) either the surface gravity, metallicity, or microturbulence velocity required fewer (more) boron atoms to minimize the χ^2_ν statistic. The choice of continuum will also affect the derived abundances. Therefore, the continuum placement was altered by $\pm 2\%$ in order to assess the uncertainty introduced by a poorly normalized spectrum. As is seen in Table 5, continuum misplacement is a very real concern in these spectra in which true continuum windows are few. Finally, since the quality of the observed spectra can have an effect on the abundances calculated, we gauged the

TABLE 5

ABUNDANCE ERROR ESTIMATES

HR Number	HD Number	Abundances log N(B)[a]	Abundances log N(B)$_N$[b]	$\Delta T_{\rm eff} \pm 100$ K	$\Delta \log g \pm 0.20$ dex	Δ[Fe/H] ± 0.10 dex	$\Delta\xi \pm 0.25$ km s^{-1}	Continuum $\pm 2.0\%$	Cayrel Formula	Total Error
235.....	4813	2.08	2.18	± 0.17	∓ 0.02	∓ 0.06	∓ 0.09	∓ 0.09	± 0.05	± 0.23
244.....	5015	1.75	1.85	± 0.15	∓ 0.02	∓ 0.03	∓ 0.07	∓ 0.07	± 0.05	± 0.19
962.....	19994	1.84	1.91	± 0.18	∓ 0.03	∓ 0.05	∓ 0.11	∓ 0.09	± 0.07	± 0.25
4501.....	101606	1.48	1.74	± 0.19	∓ 0.02	∓ 0.09	∓ 0.04	∓ 0.08	± 0.07	± 0.24
5447.....	128167	1.74	2.03	± 0.23	∓ 0.02	∓ 0.11	∓ 0.06	∓ 0.11	± 0.04	± 0.29
6212.....	150680	1.40	1.47	± 0.13	∓ 0.01	∓ 0.02	∓ 0.07	∓ 0.07	± 0.05	± 0.17
6541.....	159332	1.85	2.00	± 0.19	∓ 0.02	∓ 0.06	∓ 0.09	∓ 0.08	± 0.06	± 0.24
7469.....	185395	1.96	2.15	± 0.18	∓ 0.02	∓ 0.06	∓ 0.06	∓ 0.08	± 0.06	± 0.22
8697.....	216385	1.94	2.09	± 0.17	∓ 0.02	∓ 0.05	∓ 0.07	∓ 0.14	± 0.05	± 0.24

[a] LTE abundances.
[b] Non-LTE abundances.

uncertainty in the best-fit abundance, or, alternatively, the best-fit line strength, using the Cayrel (1988) equivalent width error estimate. This calculation provides another, independent, gauge of the uncertainty in the calculated B abundances. Each of the sources of error were combined, in quadrature, to arrive at the total error listed in the final column of Table 5.

We did not go through such elaborate procedures to find the Li and Be errors. Those errors have been estimated by an assessment of the goodness of fit of the synthetic spectra.

4.4. *Stars from the HST Archive*

As mentioned in § 2.1, we have used B observations of five stars from the *HST* archive that are in the same range of temperature and gravity. For these stars we have determined the stellar parameters using the same techniques described in § 4.1. We have new Li and Be observations for some of these stars also, as presented in Tables 2 and 3. We have taken values from the literature for the others but use our consistently derived stellar parameters. We used the Li equivalent width of <0.1 mÅ of Ferluga, Mangiacapra, & Faraggiana (1995) for Procyon and derive an LTE Li abundance of <0.05 but adopt a conservative limit of ≤ 0.50. The parameters and light-element abundances for these five stars are given in Table 6.

5. DISCUSSION

5.1. *Initial Abundances*

Our goal is to define and interpret the deficiencies of Li, Be, and B. To define a deficiency, the initial abundance must be inferred for each star. This inference is normally made from the meteoritic abundance and the run of the abundance with metallicity, as determined from abundance analyses of normal stars. The meteoritic abundances of Li and Be are taken from Anders & Grevesse (1989): log N(Li) = 3.31 $\pm$ 0.04, and log N(Be) = 1.42 $\pm$ 0.04. A redetermination of the meteoritic B abundance by Zhai & Shaw (1994) gave log N(B) = 2.78 $\pm$ 0.05, a value 0.1 dex lower than Anders & Grevesse recommended. Solar photospheric abundances are inappropriate as reference values because Li and possibly Be have been depleted, and the B abundance is poorly determined being based on the strong and blended B I 2496.8 Å line. Stellar abundances of Li and Be in normal stars have been determined for large samples, but B abundances are available for few stars.

Lithium is so highly prone to alteration of its surface abundance that it is difficult to determine how the initial Li abundance varies with metallicity. If the maximum Li abundance at a given [Fe/H] is identified as the initial Li abundance for that [Fe/H], the initial Li abundance increases with increasing metallicity (Rebolo, Molaro, & Beckman 1988b; Lambert, Heath, & Edvardsson 1991). For [Fe/H] ~ 0.0, the maximum Li abundance is similar to the meteoritic abundance. The Li plateau abundances in young open clusters, which are presumably minimally depleted (if at all), are also in agreement with the meteoritic abundance (Pleiades: Pilachowski et al. 1987; Boesgaard et al. 1988; Soderblom et al. 1993; IC 2391: Stauffer et al. 1989; IC 2602: Randich et al. 1997). Our estimates of the Li deficiency do not take into account the possible change of initial Li abundance with [Fe/H] because (1) the majority of stars in our sample have a metallicity ([Fe/H] ≈ 0) where the maximum Li abundance increases very slightly, if at all, with [Fe/H], and (2) the Li deficiencies of our Li-poor stars are so large that small corrections for inferred initial abundance are irrelevant.

TABLE 6

PARAMETERS AND ABUNDANCES FOR STARS FROM THE *HST* ARCHIVE

Name	HR Number	HD Number	log g	$T_{\rm eff}$	[Fe/H]	ξ	log N(Li)[a]	log N(Li)$_N$[b]	log N(Be)[a]	log N(B)[a]	log N(B)$_N$[b]	B/Be
α CMi	2943	61421	4.0	6560	-0.02	1.9	$\leq +0.50$	$\leq +0.50$	≤ -0.60	$+1.72$	$+1.89$	≥ 310
θ UMa.....	3775	82328	4.1	6300	-0.17	1.7	$+3.18$	$+3.05$	$+1.21$	$+2.10$	$+2.24$	10.7
χ Her	5914	142373	4.3	5810	-0.43	1.3	$+2.36$	$+2.36$	$+1.18$	$+1.91$	$+1.98$	6.3
... .	...	184499	4.1	5650	-0.75	1.5	$+1.41$	$+1.46$	$+0.68$	$+1.74$	$+1.82$	13.8
ι Peg	8430	210027	4.3	6480	-0.08	1.5	$+3.07$	$+2.98$	$+1.23$	$+2.07$	$+2.23$	10.0

[a] LTE abundances.
[b] Non-LTE abundances.

Extensive data on Be abundances in main-sequence F and G stars have been provided by Boesgaard (1976), Rebolo et al. (1988a), Boesgaard & King (1993), and Stephens et al. (1997). Additional data on old disk ([Fe/H] < -0.3) and halo stars are offered by Deliyannis et al. (1997). The Be abundance at [Fe/H] $= -1$ is less than the meteoritic value: [Be/H] ≈ -0.5 (Boesgaard 1996). Near [Fe/H] ~ 0, Be abundances increase only very slightly with [Fe/H]. In light of this evidence and of the fact that the Be deficiencies exceed 1 dex for all but two of our Li-deficient stars, we have not applied a correction to the Be abundances to take account of possible differences in initial abundances. Moreover, the Be abundances of disk stars vary from star to star with an approximate amplitude of 0.8 dex at [Fe/H] ~ 0.0 for stars that have not significantly depleted their Li (Boesgaard & King 1993). If this reflects a real variation of the initial Be abundance, there is clearly no point in making the much smaller adjustment to the adopted initial Be abundance for our stars spread over a small range in [Fe/H].

Data on stellar B abundances are sparse. Observations of the B II 1362 Å resonance line in hot stars have provided some data beginning with the survey by Boesgaard & Heacox (1978) that reported a mean LTE abundance log $N(\mathrm{B}) = 2.1 \pm 0.3$ and estimated the correction for non-LTE effects to increase this value by 50% to 2.3. New non-LTE calculations by Cunha et al. (1997) show that the abundance has to be raised: the mean abundance becomes log $N(\mathrm{B}) = 2.6 \pm 0.1$ when the three hottest stars are omitted and 2.7 ± 0.3 if they are retained. Recent observations of the 1362 Å line in four B-type stars in the Orion association give mean LTE and non-LTE abundances of 1.8 ± 0.2 and 2.7 ± 0.2, respectively (Cunha et al. 1997). The non-LTE abundances are in good agreement with the meteoritic abundance.[6]

Analyses of the B I 2497.8 Å line in F stars provides additional information. The analyses of Lemke et al. (1993) of their echelle spectra for θ UMa and ι Peg gave the LTE abundances log $N(\mathrm{B}) = 2.3$ and 2.4, respectively, which translate to the non-LTE abundances of 2.4 and 2.6 (Kiselman & Carlsson 1996). To within the errors of measurement, the mean abundance of 2.5 is consistent with the non-LTE abundances obtained for A and B stars from the B II 1362 Å line. The mean is possibly also consistent with the meteoritic abundance [log $N(\mathrm{B}) = 2.78$].

Among our sample, HR 235 was chosen as a "standard" because of its mild (-0.6 dex) Li depletion and even smaller (-0.2 dex) Be depletion; this star is most likely to have retained its initial B abundance. Our analysis gives the non-LTE abundance log $N(\mathrm{B}) = 2.18$, a value 0.6 dex less than the meteoritic abundance. Our reanalysis of the spectra of θ UMa and ι Peg gave LTE abundances of 2.17 and 2.07 using Lemke et al.'s atmospheric parameters, i.e., abundances 0.1–0.3 dex less than obtained by Lemke et al. Our non-LTE B abundances for HR 235, θ UMa, and ι Peg are identical to within 0.06 dex. The metallicities are within about 0.1 dex of solar, but the B abundances are approximately 0.6 dex less than the meteoritic value. Two stars with [Fe/H > -1 were observed by Duncan et al. (1997b): our reanalysis gives the non-LTE abundances as log $N(\mathrm{B}) = 1.98$ for χ Her with [Fe/H] $= -0.43$ and 1.82 for HD 184499 with [Fe/H] $= -0.75$. These two abundances are also less than the meteoritic abundance, but, in part, they may owe their apparent deficiency to their lower [Fe/H] and the fact that the B abundance has risen with increasing [Fe/H].

Our analyses of normal F dwarfs with [Fe/H] ~ 0 and little or no depletion of Li and Be provide a B abundance that is about 0.5 dex less than the meteoritic value and the abundance obtained from A and B stars using the B II 1362 Å line. Brief comments on this difference between B abundances are in order. The possibility of systematic errors afflicting the abundance determinations for F dwarfs should be recognized. We have already noted that Lemke et al. derived higher abundances from the same spectra but using a different model atmosphere grid, a different line list, and a different spectrum synthesis program. Our synthesis program (and others) may provide an incomplete representation of the continuous and quasi-continuous (an overlapping blanket of lines) at 2497 Å that will result in a systematic error; it is likely the programs underestimate the actual opacity and so underestimate the B abundances. It may be significant that the Fe I line at 2496.533 Å with an accurate laboratory *gf*-value (O'Brian et al. 1991) and a depth comparable to that of the B I blend in the cooler stars is not reproduced correctly unless the *gf*-value is reduced by about 0.5 dex. Of course, low excitation Fe I lines may be subject to effects—non-LTE, for example, that are not quantitatively transferable to the B I line. More simply, the B I line in these F dwarfs is a strong saturated line that would normally not be considered in an abundance analysis. Interpretation of such strong lines depends on the model representing correctly the upper photosphere, a region that may not be well reproduced by the standard assumptions behind construction of model atmospheres. A part of the abundance differences may reflect the fact that B may follow Be in showing an (apparent) intrinsic spread in abundance at a given [Fe/H].

Although the difference between our non-LTE B abundance of the standard F dwarfs—HR 235, ι Peg, χ Her, and θ UMa—and the meteoritic abundance is not fully explained, we adopt the reference B abundance as the mean of 10 stars: our seven stars, with non-LTE B abundances of 1.85–2.18, and the three archive stars, θ UMa, ι Peg, and χ Her. This value is log $N(\mathrm{B}) = 2.08 \pm 0.14$. For the purposes of this work, the true value of the initial B abundance is less important than the relative deficiencies.

5.2. *Boron in the Li-deficient stars*

Eight of our nine stars are Li deficient, and all but two have the same B abundance. The exceptions for which B is mildly less abundant are ζ Her, which is discussed below, and HR 4501. In the latter case for which [Fe/H] $= -0.74$, the appropriate reference abundance may, as noted above, be less than the meteoritic abundance. Judged by the lower reference abundance, HR 4501 has not depleted B to a measurable extent.

There is no correlation between the B abundance and variables such as effective temperature, [Fe/H], and the Li and Be abundances. In particular, the B abundance is

[6] Boron in local diffuse interstellar gas has an abundance log $N(\mathrm{B}) \simeq 2.0$ (Federman et al. 1993; Jura et al. 1996; Federman et al. 1996). This result and the stellar non-LTE abundances imply interstellar B is depleted by a factor of 4–5 through—presumably—accretion onto grains. Depletion of this severity was not expected by the simple recipes that indicate an empirical correlation between depletion and condensation temperature. It is presumably no more than a curiosity that the depletion vanishes if the LTE stellar abundance is adopted as the reference value.

unchanged as Li and Be are depleted over a range of at least 2.7 dex and 2.0 dex, respectively. Figure 6 shows the B abundances of our nine stars and the five archive stars plotted against the Be abundances. The B abundance indicated by the solid lines is the mean from our seven stars with the three from the archive and excludes HR 4501 and ζ Her A. Over a range of Be abundances extending down 1.4 dex from HR 235's abundance, B is apparently not depleted. For log N(Be) < -0.3, B is depleted if results for HR 4501 and HR 6212 are taken at face value. We suggested earlier that HR 4501's lower B abundance reflects a lower initial abundance. ζ Her A is discussed below. Figure 6 shows that there might be a hint that mild B deficiencies occur only for extreme Be deficiencies.

An alternative presentation of our results is given in Figure 7 to highlight how B differs so remarkably from Li and Be. The stars are ranked by their Be abundances. Deficiencies are calculated relative to the meteoritic abundances for Li and Be and to the mean of our total sample (excluding HR 4501, HR 6212, HD 184499, and Procyon) for B. In Figure 7 we plot the deficiencies against the ranking of the stars. The steady growth of the Be deficiency with ranking is not matched by a B deficiency. The Li deficiency in all cases exceeds the Be deficiency.

5.3. *Galactic Boron Variations*

It is of interest that the B abundances of six stars are not dependent on [Fe/H]: three stars with [Fe/H] > 0.0 give a mean non-LTE abundance log N(B) = 1.99, and three stars with [Fe/H] $\simeq -0.3$ give log N(B) = 2.03. Unless mechanisms for producing mild depletions of B are subtly more effective in metal-rich stars, it would seem that our results imply a very slow growth of Galactic B with [Fe/H] for the range [Fe/H] ≥ -0.3. The slow growth is certainly consistent with observations of Be (Boesgaard & King 1993; Deliyannis et al. 1997). Those observations also show that Be abundances range over about 0.8 dex for stars with little or no depletion of Li.

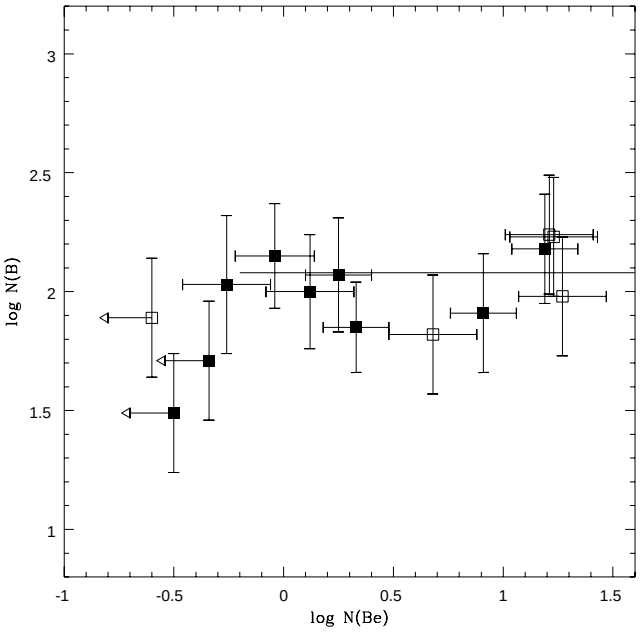

FIG. 6.—Abundances of B vs. Be with error bars. Our nine program stars are the filled squares; the open squares are the stars from the *HST* archive. The straight line at log N(B) = 2.08 is the mean of seven stars. HR 4501 and ζ Her A seem to have lower B abundances. The arrows pointing to the left indicate upper limits on the Be abundance.

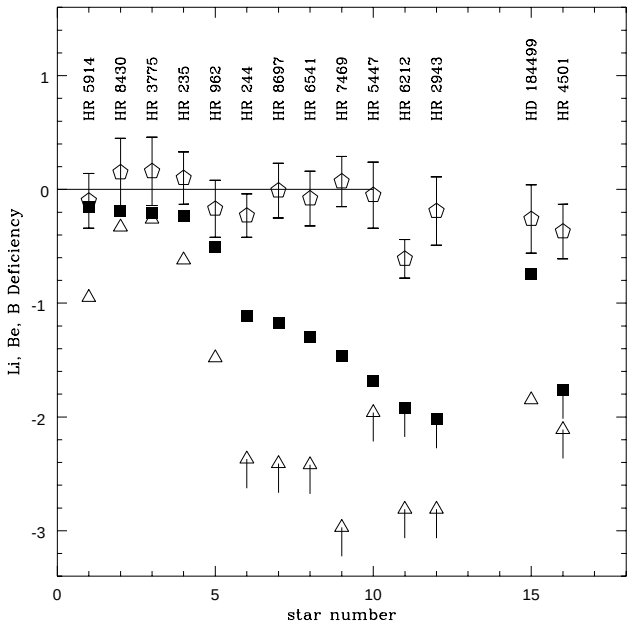

FIG. 7.—Deficiencies of Li, Be, and B plotted in order of Be deficiency. The abundances for B and Li are the non-LTE values. The open pentagons are B deficiencies, the filled squares are Be deficiencies, and the open triangles are Li deficiencies. The vertical line on some of the Li and Be points indicates an upper limit. The two stars on the right, HD 184499 and HR 4501, have lower metallicity than the others, so they have been separated. The initial values for Li and Be are the meteoritic abundances, while the mean B abundance in our seven stars is taken for the B initial value.

Figure 8 shows the B/Be ratio in our program and previously observed stars. The six stars having a range in [Fe/H] from -0.75 to $+0.15$ and a range in N(Be) from 0.7 to 1.3 (a factor of 4) *all have the same* B/Be ratio of about 10–15 to within ± 0.10 dex. For the four stars with [Fe/H] ~ 0 and little or no depletion of Li (HR 235, HR 962, θ UMa, and ι Peg), the Be and B abundances range over 0.3 dex, but the B/Be ratio is constant to ± 0.03 dex. No likely combination of errors in the analyses could contrive to reduce the errors for Be or B so greatly for that uniformity in the B/Be ratio. It seems more probable that there is a real star-to-star variation in the Be/Fe and B/Fe ratios but that the Be and B abundances are highly correlated. This is consistent with the belief that both B and Be originate in cosmic-ray interactions (see, e.g., Duncan et al. 1997a).

5.4. *Boron in ζ Her*

The lowest B abundance of the sample is that obtained for ζ Her (HR 6212). This abundance, which is about 0.6 dex less than in the rest of the sample, appears well determined. In particular, the spectrum was obtained with ECH-B. It seems unlikely that various sources of error have conspired to produce a spuriously low B abundance. The star is, however, the coolest in our sample. A deficiency in B of 0.6 dex may not be surprising in light of the fact that the star has the lowest Be abundance of the sample. The upper limit rivals that of HR 4501, also with a B abundance less than the majority of the sample.

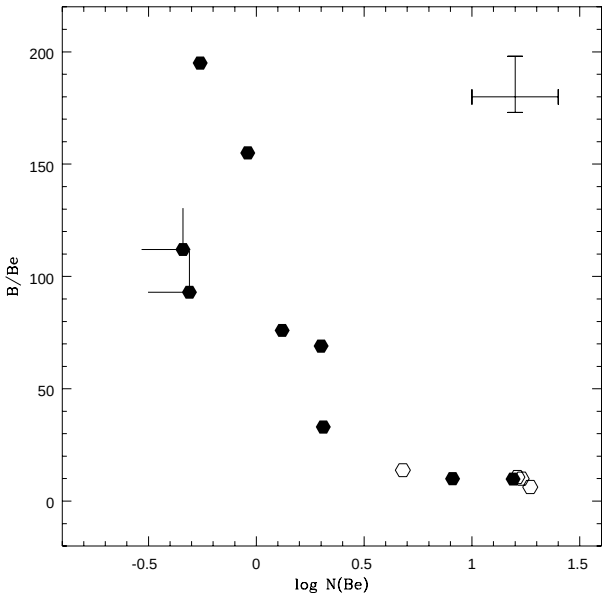

FIG. 8.—Numerical ratio of B/Be plotted against the Be abundance. A typical error bar is shown in the upper right. Our program stars are the filled hexagons, while the *HST* archive stars are the open hexagons. The two stars with upward and leftward lines have upper limit Be abundances. Note that there are six stars with B/Be ratios of ~ 10 but that have a range of a factor of 4 in Be abundance, which is apparently matched by that range in B abundance. As Be is further depleted, the B/Be ratio increases.

5.5. *Implications for Stellar Evolution*

The constancy of the boron abundances in most of the stars is rather striking in view of the large variations in Li and Be, which range from nearly normal (meteoritic) to severely underabundant (1–3 dex for Li and 1–2 dex for Be; Fig. 7). Whatever mechanism is responsible for these large Li and Be depletions has apparently left B unaffected. We discuss implications for each of the three types of mechanisms that have been proposed as the cause of the Li gap: mass loss, diffusion, and slow mixing.

5.5.1. *Mass Loss*

Although the B data alone are not inconsistent with mass loss, the mass-loss scenario is strongly argued against by the Li and Be data (Deliyannis & Pinsonneault 1993; Stephens et al. 1997). The reasons for this are as follows. Since (1) the Li and Be preservation regions have rather sharp boundaries, (2) Be is preserved to approximately twice the depth as Li, and (3) the surface convection zone (SCZ) occupies only a small fraction of these regions, any measurable deficiency of Be can occur only after all the Li is already gone. But F stars show that Be depletion occurs while Li is still present. This is especially striking in stars similar to 110 Her, in which Be is depleted by about a factor of 10, yet Li is still detected (and depleted by about a factor of 100). Stephens et al. identify 12 possible analogs of 110 Her. The mass-loss scenario is also argued against by Li observations in M67 stars evolving out of the gap (Deliyannis et al. 1996).

5.5.2. *Diffusion*

The Li data alone are no longer fully consistent with diffusion (Richer & Michaud 1993; Balachandran 1995). When Li and Be are considered together, the case against diffusion is even stronger (Deliyannis & Pinsonneault 1993; Stephens et al. 1997). Similarly, the B data are inconsistent with diffusion, as we now elaborate. In completely stable radiative layers sufficiently deep in the model stellar interior, Li and Be (and presumably B) diffuse downward via gravitational settling and thermal diffusion at roughly similar rates (Richer & Michaud 1993). The efficiency of diffusion increases with model radius but can be hindered by turbulence, even by very moderate turbulence; thus, for example, no diffusion occurs within the SCZ. On a (monotonic) isochrone, the SCZ becomes *shallower* with *increasing* $T_{\rm eff}$, so the light-element diffusion out of the base of the SCZ increases with $T_{\rm eff}$. This predicts the cool side of the Li gap. However, at about $T_{\rm eff} = 6700$ K, the base of the SCZ is sufficiently shallow (cool) so that Li retains an electron; Li can thus be radiatively accelerated into the SCZ, enriching the surface abundance. The Li abundance is predicted to rise steeply for about 100 K in $T_{\rm eff}$ and then plummet precipitously at higher $T_{\rm eff}$. Be retains an electron at a slightly higher temperature, or near the base of a deeper convection zone, so Be enrichment is predicted to begin at about 6600 K. Like Li, Be also rises initiallyand then plummets according to the theory. Presumably, this pattern repeats for B, so B enrichment might begin above roughly 6500 K. Below 6500 K, all three elements should show similar depletions. Our data show that they do not. The surface Li abundance is depleted faster than the surface Be abundance (Deliyannis & Pinsonneault 1993; Stephens et al. 1997). And even though Li and Be vary by orders of magnitude in our program stars, B is constant (Figs. 6 and 7). Our B abundances remain (nearly) constant even above $T_{\rm eff} = 6500$ K, where large variations in B might be expected. Thus, when considered together with the Li and/or Be data, the B data also argue against diffusion as the dominant mechanism. The normal Na, Mg, Si, Ca, and Sc abundances found by Boesgaard & Lavery (1986) in extremely Be-deficient F stars, including in some of the stars considered here, provide further evidence against diffusion in this context. Since diffusion *should* be important in perfectly stable layers, the absence of its signatures in our stars supports the idea that mixing occurs in these stars (see below) and that mixing inhibits the efficiency of diffusion.

5.5.3. *Slow Mixing*

Various types of slow mixing have been proposed as the origin of the Li gap. These include wave-driven mixing (García López & Spruit 1991) and mixing related to rotation, such as from meridional circulation and from instabilities triggered by differential rotation with depth (Charbonneau & Michaud 1988; Pinsonneault et al. 1990; Zahn 1992; Charbonnel et al. 1994). The efficiency of wave-mixing would increase with shallower SCZs, creating the cool side of the Li gap, and decrease with still shallower convection zones, creating the hot side. The rotation scenarios produce the cool side as a result of the increase in rotation with mass. The hot side is more challenging, since rotation rates continue to increase. The Charbonneau & Michaud (1988) scenario relies on upward radiative levitation plus finely tuned mass loss to counter the surface mixing, though it is not clear that this scenario is still viable in view of the improved diffusion calculations of Richer & Michaud (1993). The scenarios of Vauclair (1988) and Charbonnel, Vauclair, & Zahn (1992) rely on the splitting of circulation into two distinct cells for very shallow convection zones, although other complications (such as due to

diffusion) argue against this (see, e.g., Zahn 1992). Of relevance may be the occurrence of the break in the Kraft rotation curve (Kraft 1967) at the same $T_{\rm eff}$ as the Li gap. Below the break, stars are inferred to spin down during their lifetime; above, they do not. Hence, the hot side of the gap may reflect the absence of mixing, either because the lack of angular momentum loss can no longer cause mixing (Pinsonneault et al. 1990) or perhaps because the lack of a torque allows the establishment of a circulation-free state (Zahn 1992).

The signature of simultaneous Li and Be depletion would appear to be the normal depletion pattern for F stars (Stephens et al. 1997). In general, the observed Li and Be depletion pattern of stars like 110 Her, namely the pattern of a significant Be depletion even while Li is still present (though more strongly depleted than Be), is exactly what one expects from some forms of slow mixing (Deliyannis & Pinsonneault 1993).

Distinguishing between different scenarios for slow mixing is a bit more challenging but can potentially be accomplished by understanding (1) the timing of the light element depletions, (2) the detailed Li-$T_{\rm eff}$ (and, ideally, Be-$T_{\rm eff}$) morphology in clusters and its evolution and dependence on composition, (3) the light-element abundance differences at a given $T_{\rm eff}$, and (4) the evolution of Li/Be/B ratios, which probe the relative efficiency of mixing with depth. We refer the reader to Stephens et al. (1997) for detailed comparisons of the currently available Li and Be field observations to the various scenarios. They conclude that the Yale models best fit the constraints.

Although none of the slow mixing scenarios have made specific predictions for B, it is expected that the preservation of B to significantly greater depths than Be (or Li), coupled with the common feature these models have of increasing mixing efficiency toward the surface, results in little or no B depletion. At least, much more severe Be depletion must precede measurable B depletion. The (near) uniformity of the B abundance in most of our stars is thus consistent with slow mixing. The B data also argue against older models of "turbulent diffusion" in which the mixing was more uniform with depth and much more severe. The star ζ Her A, which would be about 3.4 Gyr old according to the models in Figure 1, might be illustrating (below) that B depletion does occur eventually in some (sufficiently old?) stars. Future models should assess the capability of various mechanisms to create B depletion. This may be difficult for the internal wave models, for which Li and especially Be depletion is already energetically difficult. In general, we call on future models to include predictions not only for Li and Be but also B (and $^{12}C/^{13}C$).

5.5.4. *The Mildly B-deficient Stars*

It is of relevance to determine whether or not the mild B deficiencies in HR 4501 and ζ Her A are related to the stellar mechanisms considered here. We also include Procyon in the discussion since Lemke et al. (1993) found it to be slightly B-deficient relative to θ UMa, although it is not definitively deficient relative to the adopted average B in this study. As discussed above, HR 4501 is metal poor, and its initial B abundance (and initial Be also) may have been lower than that of our standard stars. Thus, there is no evidence that it has actually suffered B depletion. By contrast, it would appear that ζ Her A has suffered a small amount of surface B depletion.

Finally, HR 244 could be included in the list of possibly slightly B-deficient stars (Fig. 7). This would be especially interesting if it were an actual B depletion, in view of the clearly more strongly depleted (yet detected) Be. Unfortunately, it is not clear whether the possible B deficiency would be an initial condition or actual B depletion. Perhaps a larger sample could resolve statistically the issue of whether measurable B depletion is possible while Be is (low but) still detectable. This star's Li is also severely depleted.

Regarding the issue of B depletion, the case of Procyon requires separate discussion. Procyon has a white dwarf companion in an eccentric orbit with a semimajor axis of about 16 AU. Mass transfer from the companion's red giant progenitor to Procyon would certainly result in Li, Be, and B deficiencies since these elements would, at the very least, be diluted in the giant. The overall evidence points to the latter, since mass transfer would necessarily alter also the C, N, and O abundances. Furthermore, if the companion had reached the asymptotic red giant branch, abundances of those elements with a dominant contribution from the *s*-process would now be enhanced. Many studies including detailed non-LTE analyses of certain elements have shown that Procyon has a solar composition to high accuracy (see, for example, Takeda 1996 for C, N, and O abundances; Kato & Sadakane 1986 and Steffen 1985 for *s*-process elements). It seems clear, as Steffen noted for Li and Be, that the light-element (including possibly B) deficiencies are intrinsic to Procyon and are not a direct or indirect (tidal mixing?) result of the companion's presence.

We now return to the main issue, namely, what is the origin of the mild B depletion in ζ Her A and the possible depletion in Procyon? Both stars are much too hot for standard subgiant B dilution to have begun. ζ Her A appears to be the most evolved and oldest star in our sample and also has the lowest Li upper limit and second lowest Be upper limit after Procyon. Figure 5 shows the spectra for the Li, Be, and B regions in this star. As discussed above, the Li and Be data point to the action of slow mixing as the dominant mechanism. Although we have argued above that slow mixing is consistent with little (immeasurably small) or no B depletion, it is also possible that slow mixing acting with sufficient efficiency and/or over sufficiently long periods of time will eventually begin to deplete B. A similar conclusion was reached by Lemke et al. regarding Procyon's possible B depletion. Another interesting possibility also deserves mention, namely that diffusion could occur in some stars at late stages in their evolution (perhaps near the turnoff) if sufficient stability has been achieved in their outer layers. Indeed, there is evidence that helium diffusion has occurred in the Sun (Guenther & Demarque 1997); ζ Her A appears to be a bit younger than the Sun. However, even if (late-time) diffusion has depleted B (and Li and Be) by about a factor of 4 in ζ Her A, the vast majority of the Li and Be depletions in this star would still require an alternate explanation (mixing?). A much larger sample size could reveal how common this B depletion is, whether it must always be accompanied by far larger Li and Be depletions, and whether more severe B depletion than the factor of 3 or so determined here is possible.

6. SUMMARY AND CONCLUSIONS

We have determined B abundances for nine Population I F dwarfs, selected on the basis of their Li and Be abundances. We have reanalyzed five other F stars that have

been observed by others and are in the *HST* archive. For most of our program stars, we have made new observations of Li and Be at high signal-to-noise ratios and high spectral resolution at the Keck I telescope, the Canada-France-Hawaii telescope, and the UH 2.2 m telescope.

The new upper limits on the Li abundances are lower than previous upper limits by 0.2–0.8 dex and are factors of 90–500 lower than the meteoritic Li abundance. All of our stars were newly observed for Be, which was *detected* in seven of the nine. The Be abundances are factors of 1.7–60 (or more) below the meteoritic Be. In all cases the Li deficiency is larger than the Be deficiency.

The B abundances that we have determined are not in agreement with the meteoritic values or the non-LTE values for A and B stars, but they are similar to the abundance of B in the interstellar medium and the LTE values for the A and B stars. In spite of the enormous deficiencies in Li and Be in our stars, the B abundances are nearly constant. And there is no difference in B between three stars with [Fe/H] $= -0.3$ and three with [Fe/H] > 0.0. These facts argue against diffusion as the cause of the Li (and Be) dip as the huge Li and Be variations should be accompanied by B variations in that scenario. The observed concomitant Be and (larger) Li depletions, as exemplified by 110 Her (Deliyannis & Pinsonneault 1993) and the large data set of Stephens et al. (1997), argues strongly against mass loss and strongly in favor of slow mixing that acts below the (very shallow) surface convection zone and has decreasing efficiency with depth. Both B isotopes are so much sturdier to reactions with protons than Li and Be and survive to significantly greater depths; the small or nonexistent B depletion in our stars thus further supports this type of mixing. Stephens et al. (1997) discuss the various scenarios in detail and favor models with rotationally induced (slow) mixing, such as the Yale models. Those models suggest little or no B depletion; we suggest that future model makers consider the B constraints as well as the Li and Be constraints.

For two stars—HR 4501 and ζ Her A—B is lower than the constant value we find for the other seven stars. Since HR 4501 has [Fe/H] $= -0.74$, it may have formed with a lower B abundance initially, so it may not have undergone B depletion, but it *has* depleted its Be. For ζ Her A the abundance of B is 0.6 dex less than the mean of the other stars. This star has the largest Be deficiency in our sample—more than a factor of 80—and a Li deficiency of more than a factor of 600. The B deficiency, accompanied by the large Li and Be deficiencies, is consistent with a slow mixing process such as rotationally induced mixing, which has acted either with greater efficiency or over a longer period of time. This 1.4 $M_\odot$ star is the most evolved star, and one of the oldest stars, in our sample and thus has had more time to deplete its light elements.

Six of the enlarged sample of 14 stars have a ratio B/Be of about 10, which is the value predicted if spallation reactions are the source of B and Be production. The range in Be for those six stars is a factor of 4. A similar range in Be was found by Boesgaard & King (1993) for stars of solar metallicity and mild, if any, Li depletion [log N(Li) > 2.5]. Correlated and comparable variations in Be and B abundances are expected if these elements are synthesized primarily by spallation reactions induced by Galactic cosmic rays. The four stars with solar metallicity in our sample show a Be range of 0.3 dex, but the B/Be ratio is constant to within ± 0.03. The observation that Be and B abundances range over a factor of 2 for a minor spread in the metallicities of the stars suggests that the production of Be and B in the Galactic disk varies relative to production of elements such as Fe by stellar nucleosynthesis.

All of our stars (with the possible exception of Procyon) originated in the Li dip region on the ZAMS. Their striking lack of B depletion indicates that the mechanism responsible for the Li and Be dip has not operated long enough or thoroughly enough to have affected the surface abundance of B.

We thank Douglas Duncan and Louisa Rebull for providing us with their reduced spectra for HD 184499 and χ Her. We are grateful to Jeremy King for his help at the telescopes with some of the Li and Be spectra and to Steven Vogt for allowing us to use some of the Keck Be spectra obtained during the commissioning time of HIRES. This research has been supported by grants from the Space Telescope Science Institute to the University of Hawaii and the University of Texas. Support for C. P. D. was provided by NASA through grant HF-1042.01-93A awarded by the Space Telescope Science Institute which is operated by the Association for Research in Astronomy, Inc., for NASA under contract NAS 5-26555, and by the University of Hawaii Foundation through the Beatrice Watson Parrent Postdoctoral Fellowship.

REFERENCES

Anders, E., & Grevesse, N. 1989, Geochim. Cosmochim. Acta, 53, 197
Bahcall, J. N., & Pinsonneault, M. H. 1995, Rev. Mod. Phys., 67, 781
Balachandran, S. 1995, ApJ, 446, 203
Blackwell, D. E., & Lynas-Gray, A. E. 1994, A&A, 282, 899
Blazit, A., Bonneau, D., & Foy, R. 1987, A&AS, 71, 57.
Boesgaard, A. M. 1976, ApJ, 210, 466
———. 1991, ApJ, 370, L95
———. 1996, in ASP Conf. Proc. 92, Formation of the Galactic Halo ... Inside and Out, ed. H. Morrison & A. Sarajedini (San Francisco: ASP), 327
Boesgaard, A. M., Budge, K. G., & Ramsay, M. E. 1988, ApJ, 327, 389
Boesgaard, A. M., & Heacox, W. D. 1978, ApJ, 226, 888
Boesgaard, A. M., & King, J. R. 1993, AJ, 106, 2309
Boesgaard, A. M., & Lavery, R. S. 1986, ApJ, 309, 762
Boesgaard, A. M., & Tripicco, M. J. 1986a, ApJ, 302, L49
———. 1986b, ApJ, 303, 724
Bonneau, D., Balega, Y., Blazit, A., Foy, R., Vakili, F., & Vidal, J. L. 1986, A&AS, 65, 27
Carlsson, M., Rutten, R. J., Bruls, J. H. M. J., & Shchukina, N. G. 1994, A&A, 288, 860
Carney, B. W. 1982, AJ, 87, 1527
Cayrel, R. 1988, in IAU Symp. 132, The Impact of Very High S/N Spectroscopy on Stellar Physics, ed. G. Cayrel de Strobel & M. Spite (Dordrect: Kluwer), 345
Chaboyer, B., Deliyannis, C. P., Demarque, P., Pinsonneault, M. H., & Sarajedini, A. 1992, ApJ, 388, 372
Chaboyer, B., & Demarque, P. 1994, ApJ, 433, 510
Charbonneau, P., & Michaud, G. 1988, ApJ, 334, 746
Charbonnel, C., Vauclair, S., Maeder, A., Meynet, G., & Schaller, G. 1994, A&A, 283, 155
Charbonnel, C., Vauclair, S., & Zahn, J.-P. 1992, A&A, 255, 191
Chmielewski, Y., Cayrel de Strobel, G., Cayrel, R., Lebreton, Y., & Spite, M. 1995, A&A, 299, 809
Crawford, D. L. 1975, AJ, 80, 995
Cunha, K., Lambert, D. L., Lemke, M., Gies, D. R., & Roberts, L. C. 1997, ApJ, 478, 211
Deliyannis, C. P. 1990, Ph.D. thesis, Yale Univ.
———. 1995, in The Light Element Abundances, ed. P. Crane (ESO/EIPC Workshop) (Berlin: Springer), 395
Deliyannis, C. P., Boesgaard, A. M., & King, J. R. 1995, ApJ, 452, L13
Deliyannis, C. P., Boesgaard, A. M., King, J. R., & Duncan, D. K. 1997, AJ, submitted

Deliyannis, C. P., Demarque, P., & Kawaler, S. D. 1990, ApJS, 73, 21
Deliyannis, C. P., King, J. R., & Boesgaard, A. M. 1996, in IAU Commission 9 International Conference on Wide Field Spectroscopy, ed. M. Kontizas, in press
Deliyannis, C. P., King, J. R., Boesgaard, A. M., & Ryan, S. G. 1994, ApJ, 434, L71
Deliyannis, C. P., & Pinsonneault, M. H. 1993, in ASP Conf. Proc. 40, Inside the Stars (IAU Colloq. 137), ed. W. W. Weiss (San Francisco: ASP), 174
Dinescu, D. I., Demarque, P., Guenther, D. B., & Pinsonneault, M. P. 1995, AJ, 109, 2090
Duncan, D. K., Peterson, R. C., Thorburn, J. A., & Pinsonneault, M. H. 1997a, ApJ, submitted
Duncan, D. K., Primas, F., Rebull, L. M., Boesgaard, A. M., Deliyannis, C. P., Hobbs, L. M., King, J. R., & Ryan, S. G. 1997b, ApJ, 488, 338
Edvardsson, B., Andersen, J., Gustafsson, B., Lambert, D. L., Nissen, P. E., & Tomkin, J. 1993, A&A, 275, 101
Federman, S. R., Lambert, D. L., Cardelli, J. A., & Sheffer, Y. 1996, Nature, 381, 764
Federman, S. R., Sheffer, Y., Lambert, D. L., & Gilliland, R. L. 1993, ApJ, 413, L51
Ferluga, S., Mangiacapra, D., & Faraggiana, R. 1995, Mem. Soc. Astron. Italiana, 66, 376
García-López, R. J., Severino, G., & Gomez, M. T. 1995, A&A, 297, 787
García-López, R. J., & Spruit, H. C. 1991, ApJ, 377, 268
Guenther, D. B., & Demarque, P. 1997, ApJ, 484, 937
Hiltgen, D. D. 1996, Ph.D. thesis, Univ. of Texas at Austin
Iglesias, C. A., & Rogers, F. J. 1991, ApJ, 371, 408
Jura, M., Meyer, D. M., Hawkins, I., & Cardelli, J. A. 1996, ApJ, 456, 598
Kato, K., & Sadakane, K. 1986, A&A, 167, 111
King, J. R., Deliyannis, C. P., & Boesgaard, A. M. 1997a, AJ, in press
King, J. R., Deliyannis, C. P., Hiltgen, D. D., Stephens, A., Cunha, K., & Boesgaard, A. M. 1997b, AJ, in press
Kiselman, D. 1994, A&A, 286, 169
Kiselman, D., & Carlsson, M. 1994, in The Light Element Abundances, ed. P. Crane (Berlin: Springer), 372
———. 1996, A&A, 311, 680
Kozhurina-Platais, V., Demarque, P., Platais, I., Orosz, J. A., & Barnes, S. 1997, AJ, 113, 1045
Kraft, R. P. 1967, ApJ, 150, 551
Kurucz, R. L. 1993, CD-ROM 23 (Cambridge: Smithsonian Astrophysical Observatory)
Lambert, D. L., Heath, J. E., & Edvardsson, B. 1991, MNRAS, 253, 610
Lemke, M., Lambert, D. L., & Edvardsson, B. 1993, PASP, 105, 468
Maeder, A. 1976, A&A, 47, 389
Magain, P. 1987, A&A, 181, 323
Michaud, G. 1986, ApJ, 302, 650
Montalbán, J., & Schatzman, E. 1996, A&A, 305, 513
Nissen, P. E. 1981, A&A, 97, 145
O'Brian, T. R., Wickliffe, M. E., Lawler, J. G., Whaling, W., & Brault, J. W. 1991, J. Opt. Soc. Am., B8, 1185
Pilachowski, C. A., Booth, J., & Hobbs, L. M. 1987, PASP, 99, 1288
Pinsonneault, M. H. 1997, ARA&A, in press
Pinsonneault, M. H., Kawaler, S. D., & Demarque, P. 1990, ApJS, 74, 501
Proffitt, C. R., & Vandenberg, D. A. 1991, ApJS, 77, 473
Randich, S., Aharpour, N., Pallavicini, R., Prosser, C. F., & Stauffer, J. R. 1997, A&A, submitted
Rebolo, R., Molaro, P., Abia, C., & Beckman, J. E. 1988a, A&A, 193, 193
Rebolo, R., Molaro, P., & Beckman, J. E. 1988b, A&A, 192, 192
Richer, J., & Michaud, G. 1993, ApJ, 416, 312
Rogers, F. J., & Iglesias, C. A. 1994, Science, 263, 50
Ryan, S. G., & Deliyannis, C. P. 1995, ApJ, 453, 819
Saxner, M., & Hammarbäck, G. 1985, A&A, 151, 372
Schramm, D. N., Steigman, G., & Dearborn, D. S. P. 1990, ApJ, 359, L55
Sneden, C. 1973, ApJ, 184, 839
Soderblom, D. R., Jones, B. F., Balachandran, S., Stauffer, J. R., Duncan, D. K., Fedele, S. B., & Hudon, J. D. 1993, AJ, 106, 1059
Stauffer, J., Hartmann, L. W., Jones, B. F., & McNamara, B. R. 1989, ApJ, 342, 285
Steffen, M. 1985, A&AS, 59, 403
Stephens, A., Boesgaard, A. M., King, J. K., & Deliyannis, C. P. 1997, ApJ, 491, 000
Takeda, Y. 1996, PASJ, 46, 53
Taylor, B. 1994a, PASP, 106, 452
———. 1994b, PASP, 106, 704
———. 1995, PASP, 107, 734
Unsöld, A. 1955, Physik der Sternatmosphären (2d ed.; Berlin: Springer)
Vauclair, S. 1988, ApJ, 335, 971
Zahn, J.-P. 1992, A&A, 265, 115
———. 1994, A&A, 288, 829
Zhai, M., & Shaw, D. M. 1994, Meteoritics, 29, 607